Study and Analysis of Anti Vibratory Passive and Active Methods Applied to Complex Mechanical System

Cédric Lopez
e-mail: cedric.lopez@aix.ensam.fr

François Malburet
e-mail: francois.malburet@aix.ensam.fr

Arts et Metiers ParisTech LSIS,
2, cours des Arts et Métiers,
13617 Aix en Provence, France

André Barraco
ENSAM LMSP,
151, Boulevard de l'Hôpital,
75013 Paris, France
e-mail: andre.barraco@paris.ensam.fr

This paper studies problematic of a mechanical system composed of different coupled parts submitted to a high speed shock and proposes analysis of anti vibratory passive and active methods based on an experimental and theoretical coupled approach. After a shock, different parts of the system oscillate. If one of them is excited at a particular frequency, such as its proper frequency, important oscillations appear and can lead to the deterioration of the system by introducing important stresses. In this paper, we propose an analysis in order to understand this kind of problem and what we can do to avoid it. Firstly, we discuss problematic and we expose the studied system. In a second time, we develop two approaches of modeling that allow us to understand the phenomenon by carrying out numerical simulations. Then cross checking of model is completed via experimental study on drop test bench. Passive minimization method of vibrations based on experimental and theoretical coupled approach is exposed. Finally, a comparative analysis of different methods of control and experimental results of controlled system are presented. [DOI: 10.1115/1.4005236]

Keywords: control, cross check, test bench, excitation, high speed shock, mechanical coupling, minimization, nonlinear modeling, oscillations, PID, sliding mode

1 Introduction

In many applications, several mechanical systems are submitted to high speed shock; making it important to study the behavior of different parts of these systems. For example, the problem occurs in the daily life when you ride on a pothole. Your body is mechanically coupled with the vehicle. Internal organs oscillate and if they are excited at a particular frequency, you are sick. This notion is very important in the domain of transports and leads to the driving comfort. Many studies analyze this aspect and study the suspension system of vehicles because it is responsible for driving comfort as it carries the vehicle body and transmits all forces of excitations between the vehicle and the road. In fact in their study, Fischer and Isermann [1] analyze the role of each component of a suspension and propose active methods in order to insure comfort of passengers. Lin and Kanellakopoulos [2] not only take into account the comfort of passengers, they propose a dual objective dealing with comfort and driving safety. In fact, the stability of system submitted to shock is also to take into account.

Moreover, in an industrial context, machining is also concerned by the study of high speed shock on a mechanical system composed of different coupled parts. In fact, the problem appears when the tool impacts the piece, and the shock excites the tool holder. Xu [3] shows that vibrations induced by shock can dramatically reduce machine life and machine performance.

Aeronautics is another domain where it is important to study the behavior of an excited system. In fact, progress in the domain of materials leads frames of aircrafts to be lighter. These ones easily bend under an excitation. In his work, Kruger [4] shows that during taxiing, the fuselage is submitted to excitations leading to uncomfortable situation for passengers and stressful vibrations for the frame of the aircraft. In his study, Ghiringhelli proposes anti vibratory semi active mean [5]. Moreover, aircrafts are particularly constrained during a landing and especially a hard landing which is equivalent to a high speed shock. Because of the mechanical coupling existing between the fuselage and the landing gear, the frame of the aircraft bends and too important deformations, resulting of a particular excitation of the frame, can lead to the deterioration of the aircraft. The tail beam being the most critical part will be particularly studied.

The selection of an appropriate model of the structure is crucial, since it determines the complexity of the control design and parameter tuning process. Some paper presents a flexible model-free control structure based on physical insights in the structure [6,7]. Finite elements with different orders can be used in the analysis of constrained deformable bodies that undergo large rigid body displacements [8]. It is the case for the landing of an aircraft [9]. In order to analyze problematic and to understand the phenomenon, we propose to use analytical and multibody dynamics approaches.

We suggest studying the behavior of a mechanical system composed of different subsystems mechanically coupled and submitted to a high speed shock. The studied system is composed of three series connected sprung subsystems. Each subsystem represents different parts of aircraft like wheel, fuselage with landing gear and tail beam. High speed shock is produced by the impact on the ground of the system following its free fall. The behavior of the upper part of the system is particularly studied because it represents the tail beam of an aircraft and so we want to understand and to avoid its oscillations.

Thus, through one analytical model and one multibody model, we firstly carry out numerical simulations using a Runge-Kutta [2,3] integration scheme with variable step time that allow us to understand phenomenon. In second time, we present experimental set up allowing us to cross check model. Then, we exposed passive method of minimization of vibrations based on an experimental and theoretical coupled approach. Finally, a comparative analysis of different controllers with description of real controlled device and its experiment are presented.

Manuscript received June 20, 2007; final manuscript received June 15, 2011; published online January 17, 2012. Assoc. Editor: Claude-Henri Lamarque.

2 Modeling

The studied system is composed of system which is equivalent to a quarter part of a vehicle with another sprung mass located on the upper mass of the quarter part of a vehicle.

The quarter part of a vehicle is composed of a wheel, an unsprung mass (*mns*) and a sprung mass (*ms*) linked by a suspension (cf. Fig. 1 and Fig. 5). These two coupled subsystems represent the fuselage of an aircraft with a wheel type landing gear.

The upper subsystem located on the sprung mass of the quarter part of the vehicle, is composed of a mass (*mq*), a spring and a damper. Mechanically equivalent to a tail beam, its damping rate has been firstly set to 3%, which almost corresponds to a structural damping rate.

We have a free fall of the system; so the speed of the shock is proportional to the height of the fall. Here, we study a shock with a speed of 2.8 m/s. The height of the fall is 0.4 m. In all following simulations, initial conditions on positions of different masses making up the system, allow us to adjust the speed of the shock.

First of all, we develop an analytical linear model of the system. Then we present a multibody approach corresponding to a numerical non linear model based on experimental definitions of some different constitutive parts of the system such as the tire and the damper of the suspension.

2.1 Analytical Model

2.1.1 Modeling. The studied system is described by the following Fig. 1.

We consider four degrees of freedom which are *Zms*, *Zmns*, *Zp* and *Zq*. Setting conditions on the absolute displacement of the point P, which corresponds to the bottom point of the tire, allow us to differentiate the phase of free fall and the phase of contact with the ground during simulations.

In fact, we have following conditions:

$Zp > 0$, phase of fall.
$Zp \leq 0$, phase of evolution of the system on ground.

In the test bench, we use springs for the stiffness of the suspension and the stiffness of the upper system. In the model, these elements are modeled by linear springs with stiffness *ks* and *kq*, respectively. Moreover, we model the tire by a linear spring with stiffness *kp*. Damping forces are modeled by linear viscous terms.

The behavior of the system is described by the following equations:

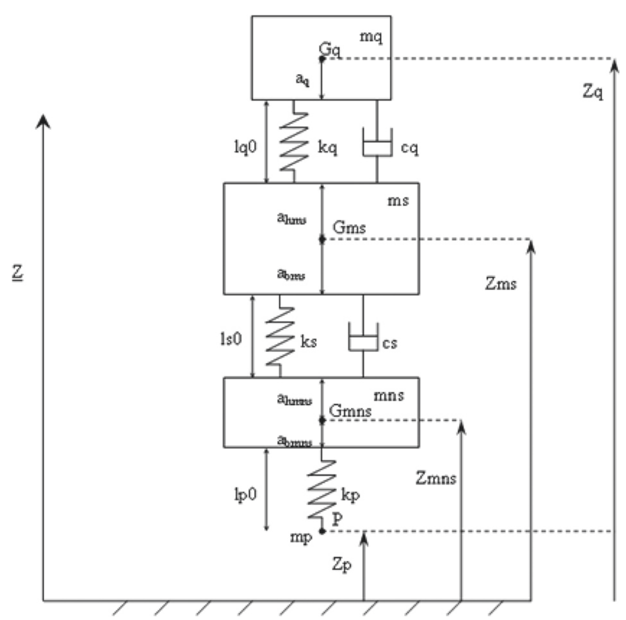

Fig. 1 Modeling and definition of parameters

$$mq \cdot \ddot{Z}q = -mq \cdot g - kq \cdot (Zq - Zms) - kq \cdot (-a_q - a_{hms} - lq0) - cq \cdot (\dot{Z}q - \dot{Z}ms) \quad (1)$$

$$ms \cdot \ddot{Z}ms = -ms \cdot g + kq \cdot (Zq - Zms) + kq \cdot (-a_q - a_{hms} - lq0) + cq \cdot (\dot{Z}q - \dot{Z}ms) - ks \cdot (Zms - Zmns) - ks \cdot (-a_{bms} - a_{hmns} - ls0) - cs \cdot (\dot{Z}ms - \dot{Z}mns) \quad (2)$$

$$mns \cdot \ddot{Z}mns = -mns \cdot g + ks \cdot (Zms - Zmns) + ks \cdot (-a_{bms} - a_{hmns} - ls0) + cs \cdot (\dot{Z}ms - \dot{Z}mns) - kp \cdot (Zmns - Zp - a_{bmns} - lp0) \quad (3)$$

$$mp \cdot \ddot{Z}p = -mp \cdot g + kp \cdot (Zmns - Zp) + kp \cdot (-a_{bmns} - lp0) \quad (4)$$

The mass *mp* is set to zero. When $Zp > 0$, the system is falling, the tire represented by the spring with stiffness *kp* does not apply any force on the mass *mns*.

2.1.2 Simulations and Analysis. We study a high speed shock. The speed of the shock is determined by the height of the fall, i.e., initial positions of different masses. Here, we analyze a shock with a speed of 2.8 m/s (a 0.4 m high fall). Moreover, we set the following condition; no bounce of the system can occur. This is a condition of stability for an aircraft during landing or a condition of safety for a car riding on a chaotic road.

The upper system composed of the mass *mq*, the spring *kq* and the damper *cq*, has a low proper frequency about 7.5 Hz

The damping coefficient (*cs*) of the suspension is different between the phase of compression and the phase of extension. This difference makes the suspension softer and guaranties no bounce.

After several simulations, we chose a damping rate of 60% for compression and 90% for extension. The damping rate, noted ξ, is calculated as following:

$$\xi = \frac{cs}{2 \cdot \sqrt{ks \cdot ms}} \quad (5)$$

The stiffness of the spring *kp* modeling the tire is set to 250 000 N/m. This is an average value for the tire used in the test bench.

We obtain the following result of simulation, as shown in Fig. 2. The impact occurs at the time 0.28 sec, outlined in Fig. 2 and on following figures by a red vertical dashed line. Moreover, on following figures, in order to improve visibility, we zoom on

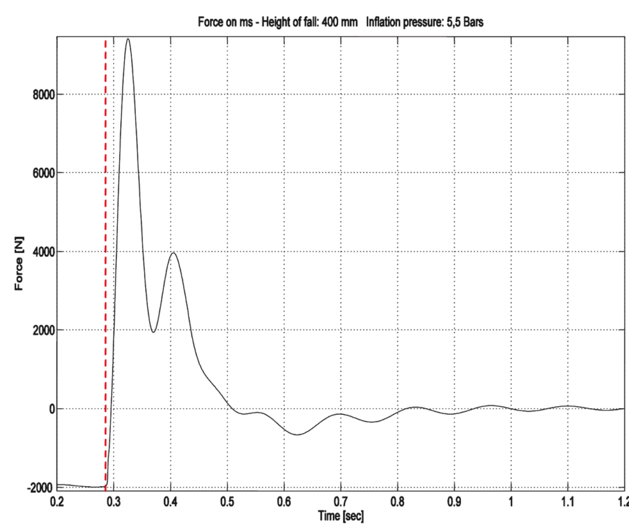

Fig. 2 Excitation force on *ms* - Analytical model

occurrence time of the impact which is calculated in function of the height of the fall. As soon as the impact occurs, we notice the presence of a double bump. The first peak depends on characteristics of the suspension. The second peak depends on the stiffness of the tire. The stiffer these elements are, the higher the peaks are. The duration of the double bump is equal to 0.13 sec. Because the mechanical coupling between the mass *ms* and the mass *mq*, the double bump excites the upper system in a frequency band near its proper frequency. The duration and the particular shape of the excitation transmitted by the suspension and resulting from the high speed shock are responsible for important displacements of the mass *mq*. Important oscillations of the upper mass *mq* (tail beam) generate important stress in the frame of the aircraft and lead to its deterioration. Thus, in order to minimize important oscillations of the upper system (*mq*), which can lead to deterioration of the frame on real aircraft, we have to control the transmitted excitation force.

Excitation force is transmitted by the suspension (landing gear); thus to control the dynamic behavior of the suspension allows us to minimize oscillations of the mass *mq*. In the following, passive and active methods of control of the dynamic behavior of the suspension are studied. Experimental results of passive mean and numerical results of simulations of active mean are exposed. This first analytical linear model allows us to understand the phenomenon. We obtain good results, but we do not take into account nonlinearities of subsystems making up the studied system. Thus, in order to have a more accurate model describing behavior of the system used in the drop test bench, we develop the following multibody approach consisting in a numerical nonlinear model based on experimental definitions of elements.

2.3 Multibody Approach: Nonlinear Model

2.3.1 Modeling. A multibody approach allows us to use parametric subsystems in order to develop a complete system with required details for each one. Moreover, kinematics have exact formulation within the chosen idealization of the real system; as a result we have a virtual prototyping system. Each part is modeled separately and then the assembly is realized.

In the real system of the test bench, the stiffness of the suspension (*ks*) and the stiffness of the upper system (*kq*) are realized by mechanical springs. Linear models used in order to describe the behavior of these elements are correct. Nevertheless, the tire and the damper of the suspension have to be accurately modeled. In fact, these two elements have a nonlinear behavior.

Tire: the implemented tire model is developed from tests.

We exert a controlled load on the tire and its stroke is measured for different pressures of inflation. The experimental law, giving the stiffness force in function of the stroke, is implemented in the model of the tire.

Damper of the suspension: the damper model is developed from a rod element with a particular experimental law issued from characterization tests.

We submit the real shock absorber to sinusoidal displacement with various frequency and we measure the corresponding damping force.

The resulting experimental law gives the damping force in function of the shock absorber stroke. This law is implemented into the damper model taking into account nonlinearities from throttling. In fact, we use a hydraulic shock absorber. Moreover, four tuning parameters allow us to modify the characteristic damping curve; in order to differentiate and to adjust damping rates of phases of compression and extension.

We have the following multibody model, as shown in Fig. 3.

2.3.2 Simulations and Analysis. Same initial conditions of simulations than those of previous simulations of linear model are set. Simulations give (see Fig. 4).

We notice a double bump whose duration is almost the same as the previous one in the analytical model (cf. Figure 4). Thus, the upper system is also excited on a frequency band near its proper frequency.

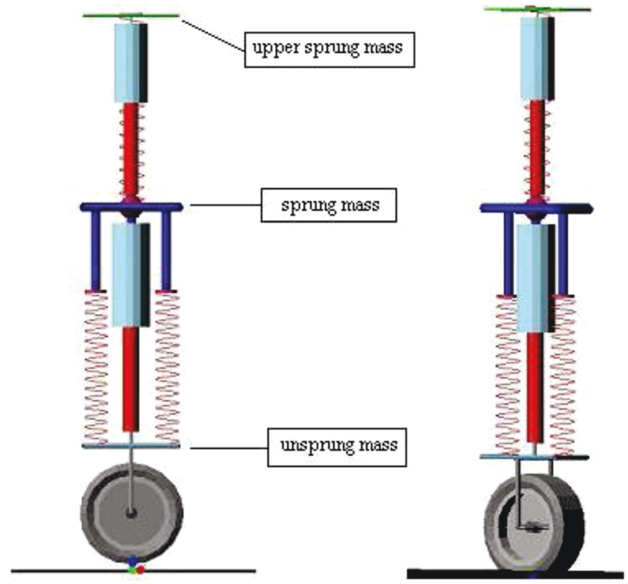

Fig. 3 Multibody model of studied system

The offset between results of simulations of the two models is small. In fact, simulations have same curve shapes and same levels of amplitude leading to a same behavior of the system. Nevertheless amplitudes of peaks of the double bump on multibody model are bigger than those of linear model. These differences can be firstly explained by the offset of damping rates between theoretical model and real shock absorber, leading to difference of amplitude on first peak. In a second time, difference of amplitude on second peak is a result of tire stiffness which is more important on real device than on linear model. Moreover, friction forces are taken into account in the multibody model through experimental characterization of the shock absorber. Friction terms can also justified the phase difference occurring between curves after the double bump.

Multibody model is more accurate than the linear one, because it is made from experimental characterization of real subsystems used on drop test bench. But according to the small offset existing between the simulations results of two models, real nonlinear

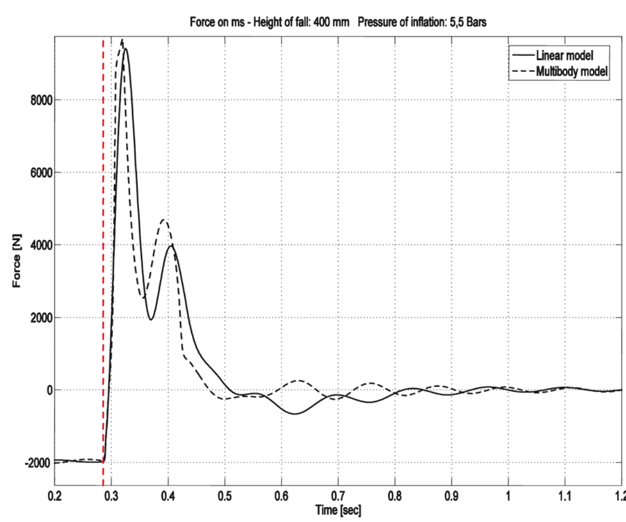

Fig. 4 Excitation force on *ms* - Comparison between analytical model and multibody model

system can be linearized. Thus, in the following of the study we will use the linear model. In fact it gives to us a good first prediction of the behavior of real system on drop test bench. Moreover, its simplicity allows us to easily cross check model from experimental results and to easily design passive and active methods in order to minimize oscillations of upper mass *mq* and its resulting forces.

In the following part, cross checking of model from measures is presented. This allows us to have a more accurate model of the real system used on drop test bench.

3 Experimental Set Up

3.1 Description. Free falls of the system are performed on a drop test bench internally designed and realized by the laboratory.

The test bench is composed of a static part and a mobile part. Two columns and a base make up the static part. The mobile part is composed of the quarter part of a vehicle (wheel, suspension, sprung mass (*ms*) and unsprung mass (*mns*)) and the upper system (mass *mq*, spring). A ball-bearing runner insures the guide of the mobile part and the shock is purely vertical. The maximum admissible height of fall is 0.76 m (distance between the bottom of the tire and the ground) leading to a speed shock of 3.9 m/s.

The stiffness of the suspension is insured by two parallel linear springs. Damping is insured by a hydraulic shock absorber whose maximal stroke is 0.3 m. Four tuning parameters on shock absorber, allow us to modify the characteristic damping curve, in order to differentiate and to adjust damping rates of phases of compression and extension.

The wheel used is a wheel of an industrial vehicle, selected because its capacity to support heavy loads.

Frequential similitudes between a real aircraft and the test bench have been made on each subsystem. Test bench is represented in Fig. 5.

Accelerometers set on each mass insure the knowledge of accelerations. Speeds and displacements are determined by numerical integrations. A force transducer between the shock absorber and the sprung mass (*ms*) measures the force transmitted by the damper. A linear inductive displacement transducer gives the stroke of the suspension. Thus, data redundancy of stroke of the suspension is insured. Processing of data is carried out via a computer with acquisition card.

Fig. 5 Drop test bench

3.2 Experimental Analysis: Cross Checking of Model. Previously, we have exposed multibody model defined from experimental characterization of subsystems making up the studied system on drop test bench. We have seen that this nonlinear model can be linearized and allows us to understand phenomenon and to give a good first prediction of behavior of system on drop test bench. Nevertheless, there are friction forces and damping forces on drop test bench which are not taken into account in previous model and other parameters of the model which need to be refined.

In order to proceed to cross checking of model, we complete several drop tests with different heights of fall. Different sensors previously described and set on drop test bench, give us measures of accelerations of each mass, measures of transmitted force by shock absorber and measures of the stroke of the suspension.

From acceleration measures of each mass, damping rates of each subsystem are determined by graphical method of logarithmic decrement.

According to this method, the damping rate of upper sprung system is estimated to 7% in comparison of its damping rate set to 3% in the previous model.

The damping rate of the suspension for compression and extension phases are almost the same as these ones of the model

Cross checking process has been completed in order to obtain a model giving simulations which are the nearest of measures of maximum configurations of drop tests.

We have the following result on acceleration of the upper sprung mass *mq* (see Fig. 6).

On Fig. 6, despite of the shift existing between the two curves, cross checking is correct. In fact, the curves have same shapes and same levels of amplitude. The observed offset is explained by friction in the ball-bearing runner.

In this study, we want to minimize the oscillations (leading to force) of the upper mass (*mq*) and most particularly the amplitude of the first peak of acceleration of *mq* via the control of the dynamic behavior of the suspension. To this end, analysis of the stroke of the suspension gives us precious data. In fact, we can observe the damping behavior of the suspension during compression and extension. Moreover, we can adjust the stiffness of suspension according to static value.

Cross checking lead to the results seen in Fig. 7. In Fig. 7, rise phase and descent phase, respectively, correspond to compression phase and extension phase. Here the model and the measure have same shape and same amplitude. Gradient of rise phase is the same in the two curves. Suspension behavior during compression phase is the same. Gradient of descent phase in concavity areas of curves is less important on model than on measure. Maximum

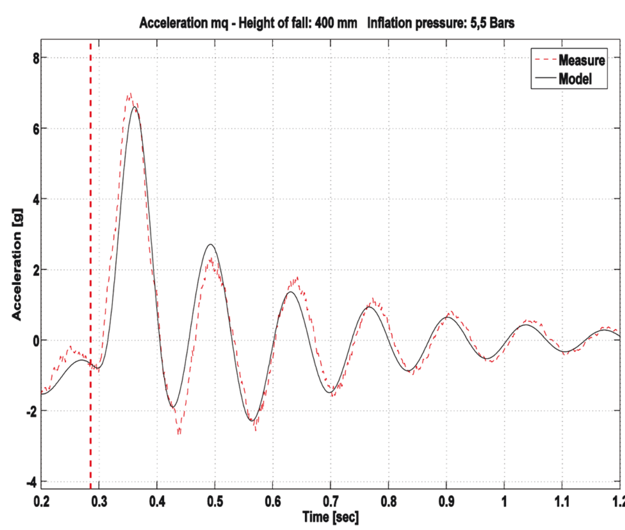

Fig. 6 Cross checking results - acceleration of *mq*

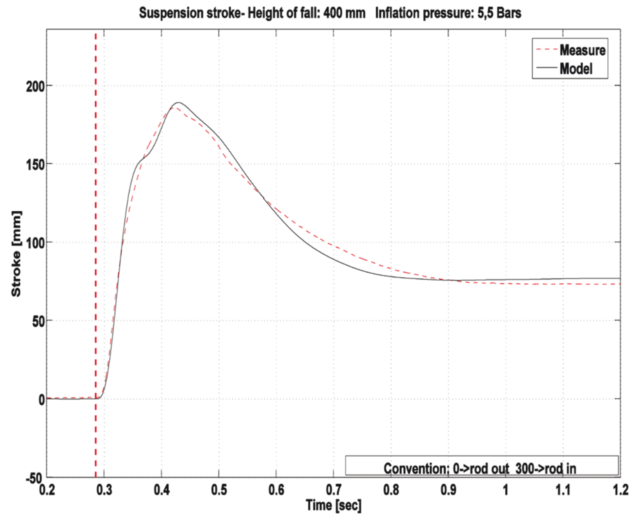

Fig. 7 Cross checking results - suspension stroke

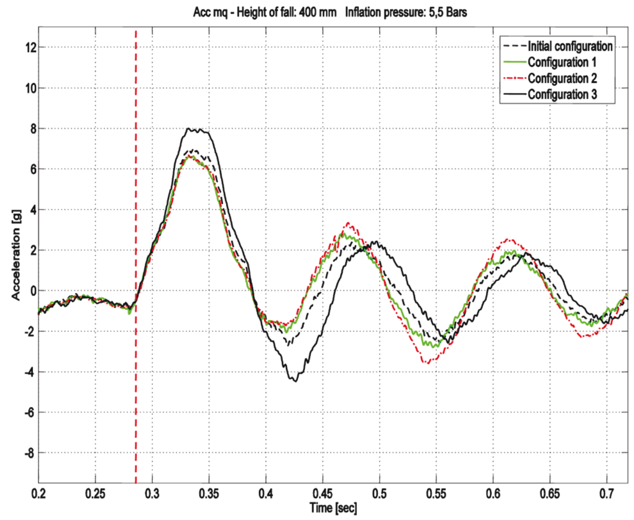

Fig. 8 Passive optimization - measured acceleration *mq*

stroke of model is smaller than measured stroke. Moreover, static stroke of model is more important than measured static stroke. Nevertheless, the offset is insignificant.

This experimental analysis allows us to complete cross checking of model from measurement on drop test bench. Thus, we have an accurate model giving us good prediction of behavior of real studied system.

We proposed in the following, an analysis of passive and active methods based on experimental and theoretical coupled approach in order to minimize first peak on acceleration of the upper sprung mass *mq*.

4 Analysis of Antivibratory Passive and Active Methods

As we previously see, important oscillations of the upper sprung mass lead to important force. During landing of aircraft, important oscillations of tail beam may cause its break.

Thus, oscillations and more precisely the resulting forces have to be minimized. The first peak of force occurring at the impact is the most critical. In the following, we study different means of minimization of the first peak of acceleration of the upper mass *mq* that is directly proportional to force.

4.1 Passive Method: Experimental and Theoretical Coupled Approach. In a passive way, we can make the upper system more rigid. For example in order to make rigid a structure, we can add stiffeners. These stiffeners displace the proper frequency of the system, making it robust to a well identified band of frequencies of excitation. But in particular domain like in aeronautics, the weight of the structure is very important. So this method cannot be used. As we previously concluded, the mechanical coupling between the sprung mass and the upper sprung mass, associated to the particular shape of the excitation force lead to oscillations of the upper sprung mass. Thus, we propose to control dynamic behavior of suspension which transmits the excitation force to the structure.

A suspension is defined by two parameters: stiffness and damping. In landing gear, stiffness is insured by pressured gas and damping is insured by throttling of oil. In our drop test bench, in order to simplify the system and to distinguish the influence of each parameter, we have physically dissociated stiffness, insured by linear springs, and damping, insured by hydraulic shock absorber. Control the excitation force via stiffness is difficult for our case. However we can adjust characteristic of damping. In fact, there are different technical devices on shock absorber allowing us to tune its characteristic damping law.

An experimental and theoretical coupled approach has been developed. In fact, we complete parametric study via simulations of model, in order to determine an optimal law of damping. Then theoretical approach is tested on drop test bench. Currently, damping force is only proportional to sinking speed. Here, we consider damping force proportional to sinking speed and proportional to sinking position of the rod of the shock absorber. This way is possible via particular hydraulic devices used on shock absorber.

We obtain the following experimental results seen in Figs. 8 and 9. In Fig. 8 and Fig. 9, we present some results of different configurations of shock absorber which are more significant. Initial configuration is compared to three others configurations. Configurations 1 and 2 are satisfying; configuration 3 is unsatisfying. In fact, configurations 1 and 2 lead to minimization of 7% of first peak of acceleration of upper sprung mass (*mq*). In configuration 3, first peak of acceleration is more important than one of initial configuration.

Here, we have modified parameters of damping in order to optimize the dissipation of energy. Optimization strategy is based on trade-off between force damping and stroke of suspension. Our approach consists in using maximum stroke in order to dissipate energy whatever landing case is. This is can be noticed on Fig. 9 with increase of stroke for configurations 1 and 2. The increase of stroke justifies diminution of the damping force at impact which

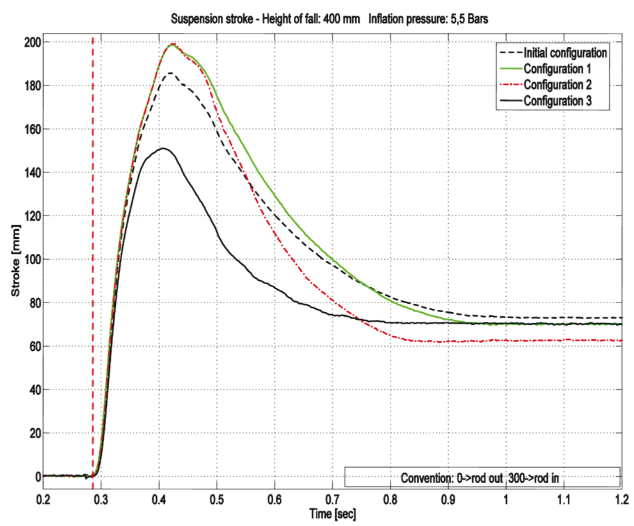

Fig. 9 Passive optimization - measured stroke

leads to a minimization of first peak of acceleration of *mq*. Moreover, the energy of impact which has to be dissipated is constant. The minimization of the damping force also leads to the increase of duration of the double bump observed on Fig. 2 and on Fig. 4. Thus, the double bump does not excite the upper mass *mq* in a frequency band near its proper frequency.

Proposed passive method is validated and leads to minimization of the first peak of acceleration. Nevertheless, minimization rate can be increased.

4.2 Active Method. The previous work shows that passive method leads to minimization of 7% on the first peak of acceleration of the upper sprung mass (*mq*). Minimization is not sufficient. In this part we propose comparative study of active means.

Several studies propose different controlled suspensions in order to minimize the acceleration of the mass *ms* ([10–12]).

The aim of all these studies is to minimize the acceleration of the mass *ms* in order to insure the comfort of passengers. Our aim is to minimize first peak of acceleration of the upper mass *mq*. No cost function was used. In fact, according to the coupling between the sprung mass (*ms*) and the upper mass (*mq*), we will control the transmitted force on *ms* in order to minimize acceleration of the mass *mq*. In fact, we cannot add a control force on the upper system; that would mean a collocated actuator on the tail beam of aircraft. This is less practicable than control landing gear.

4.2.1 Comparative Analysis of Different Methods of Control. Here we compare different methods of control. First we study two classical methods of proportional integral differential (PID) with feedback on *ms* measure of acceleration and then on *mq* measure of acceleration in order to respectively minimize acceleration on *ms* and on *mq*. Then we design sliding mode controller with state feedback on *ms* using the existing coupling between the sprung mass (*ms*) and the upper mass (*mq*) in order to minimize the acceleration of *mq*.

We want to control the excitation force transmitted by the suspension to the sprung mass (*ms*). We introduce a control force, noted u, in the equations defining the system. This force is added on the sprung mass in parallel with passive force of damping and stiffness. According to Eqs. (2) and (3) previously exposed we obtain:

$$\begin{aligned} ms \cdot \ddot{Z}ms = & -ms \cdot g + kq \cdot (Zq - Zms) + cq \cdot (\dot{Z}q - \dot{Z}ms) \\ & + kq \cdot (-a_q - a_{hms} - lq0) - ks \cdot (Zms - Zmns) \\ & - ks \cdot (-a_{bms} - a_{hmns} - ls0) - cs \cdot (\dot{Z}ms - \dot{Z}mns) + u \end{aligned} \tag{6}$$

$$\begin{aligned} mns \cdot \ddot{Z}mns = & -mns \cdot g + ks \cdot (-a_{bms} - a_{hmns} - ls0) \\ & + ks \cdot (Zms - Zmns) + cs \cdot (\dot{Z}ms - \dot{Z}mns) \\ & - kp \cdot (Zmns - Zp - a_{bmns} - lp0) - u \end{aligned} \tag{7}$$

4.2.2 Design of PID Controller. Considering the Laplace domain, the transfer function used for the PID controller is the following:

$$H(p) = \frac{U(p)}{\varepsilon(p)} = K_p \cdot \left(1 + \frac{1}{T_i \cdot p} + \frac{T_d \cdot p}{a \cdot T_d \cdot p + 1}\right) \tag{8}$$

Where K_p, T_d, T_i and a are tuning parameters determined from simulations. $\varepsilon(p)$ is the offset between the set point and the measure of the considered parameter.

We study two approaches. First, we minimize the acceleration of the sprung mass (*ms*). On a second time, we minimize the acceleration of the upper mass (*mq*). In fact, we firstly minimize the acceleration of the sprung mass (*ms*) because according to mechanical coupling between the two masses, we want to analyze the behavior of the upper mass (*mq*) using a PID controller in order to minimize the acceleration of the sprung mass (*ms*). Then we use the same PID controller with minimization of the upper mass (*mq*), always exerting the control force u on the sprung mass.

Results of the simulations of these two controlled systems are discussed in the following of this paper.

4.2.3 Design of Sliding Mode Controller. Always using the mechanical coupling between the sprung mass (*ms*) and the upper mass (*mq*), we control the behavior of the sprung mass (*ms*) using a sliding mode controller in order to minimize the acceleration of the upper mass (*mq*).

In this part, we develop the design of the sliding mode controller. We have the following state vector:

$$\underline{x} = \begin{bmatrix} Zq \\ Zms \\ Zmns \\ \dot{Z}q \\ \dot{Z}ms \\ \dot{Z}mns \end{bmatrix} = \begin{bmatrix} x_1 \\ x_2 \\ x_3 \\ x_4 \\ x_5 \\ x_6 \end{bmatrix} \tag{9}$$

In order to design the sliding mode controller, we explain the system model as an affine system of the form:

$$\dot{\underline{x}} = \underline{f}(\underline{x}) + \underline{g} \cdot u \tag{10}$$

Using this form, we can write:

$$\begin{aligned} x_4 &= \dot{x}_1 \\ \dot{x}_4 &= f_4(x_j) \end{aligned} \tag{11}$$

$$\begin{aligned} x_5 &= \dot{x}_2 \\ \dot{x}_5 &= f_5(x_j) + g_5 \cdot u \end{aligned} \tag{12}$$

$$\begin{aligned} x_6 &= \dot{x}_3 \\ \dot{x}_6 &= f_6(x_j) + g_6 \cdot u \end{aligned} \tag{13}$$

Where $j = 1 \ldots 6$.

We consider the desired state x_2^d. The error between the current and the desired state can be written as:

$$e = x_2 - x_2^d \tag{14}$$

Here, we consider the sliding surface s defined for second order system by:

$$s = \dot{e} + \lambda \cdot e \tag{15}$$

λ sets the dynamic in the sliding phase ($s = 0$). The control force u must be chosen so that trajectory of the state approaches the switching surface and then stay on it for all future time; guaranteeing stability and convergence to desired state. It is compound of a sum of two terms as following:

$$u = u_{eq} + u^* \tag{16}$$

The first term called equivalent control, is defined according to parameters of the nominal system. It is expressed as:

$$u_{eq} = g_5^{-1} \cdot \left(\ddot{x}_2^d - \lambda \cdot \dot{e} - f_5(x_j)\right) \tag{17}$$

The second term is defined in order to tackle uncertainties and to introduce reaching law. It is defined by:

$$u^* = g_5^{-1} \cdot (-k \cdot s) \tag{18}$$

The parameter k is chosen by the designer in order to define a reaching rate

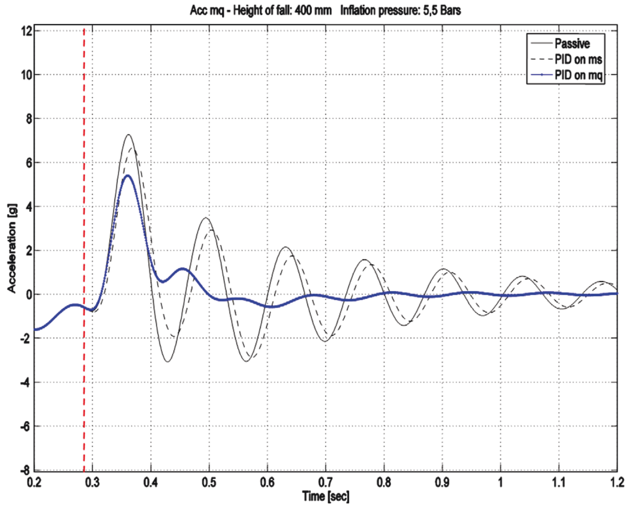

Fig. 10 Acceleration of the mass *mq* - comparison between passive and PID controllers

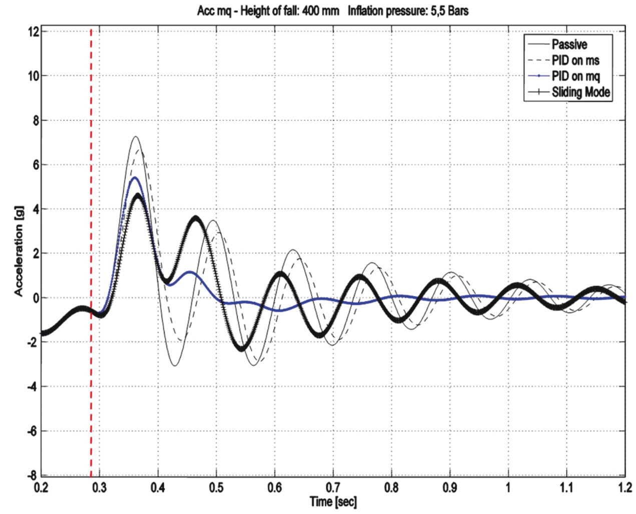

Fig. 11 Acceleration of the mass *mq* - comparison between passive, PID and Sliding mode controllers

Thus, we obtain the following law of control:

$$u = g_5^{-1} \cdot \left(\ddot{x}_2^d - \lambda \cdot \dot{e} - k \cdot s \right) \tag{19}$$

Results of the simulations of this controlled system are discussed in the following part.

4.2.4 Analysis of Simulations Results. Simulations of previous designed controllers lead to the results seen in Figs. 10 and 11.

The critical point occurs at the landing during the first compression of the landing gear. In fact, we want to minimize the amplitude of the first peak on the acceleration.

In Fig. 10, we compare the passive system with PID controllers minimizing the acceleration of *ms* and *mq*. The minimization of acceleration of *ms* using PID is not effective on the minimization of the acceleration of *mq*. Nevertheless, minimization of acceleration of *mq* using the same PID is effective. In fact we have respectively a decrease of 9% and 25% in comparison with the passive system.

In Fig. 11, we compare the passive system with PID and sliding mode controllers. Here, minimization of *ms* using sliding mode controller in order to minimize the acceleration of *mq* is very significant. We notice a reduction of 35% in comparison with the passive system on the first peak of acceleration of the upper mass (*mq*).

Moreover, in order to guaranty the stability of the system and to optimize the behavior in minimization of the acceleration of *mq*, the sliding mode controller is operative only at the impact of the system on the ground and during a defined time corresponding to the proper period of the upper system. This characteristic allows the maximum minimization of the first peak of the acceleration of the upper system (*mq*).

Thus, using mechanical coupling, in order to minimize the acceleration of the upper mass (*mq*), the sliding mode controller is the most effective in order to minimize the acceleration of the upper mass (*mq*).

4.2.5 Description and Tests of Real Controlled Device. On the real device as we previously saw, we cannot add an actuator in parallel on the passive suspension. In order to guaranty the maximum of stability and to follow the control force u, we keep a passive hydraulic shock absorber dissipating the maximum of the shock energy; and we add a controlled throttling device dissipating the rest of the energy in order to follow the desired excitation. Here, the controlled throttling device is a proportional servo valve.

The device is a semi active device where only the damping coefficient of the hydraulic shock absorber of the suspension is modified. Such a device does not need a lot of energy and moreover in case of failure of the controller, the stability of the system is thus insured.

The semi active controller is composed of two steps. The first step consists in determine the target control force u from measures on drop test bench via feedback controllers which are previously designed and exposed in this paper. The second step consists in calculate the supply current of proportional servo valve. In order to determine it, an inverse model of proportional servo valve was developed. In fact, the inverse model calculates supply current corresponding to desired target control force.

In the following, we present results of experiments of semi active for a shock with a speed of 2.8 m/s (a 0.4 m high fall). The PID controller with minimization of acceleration of the upper sprung mass (*mq*) is chosen in order to determine the target control force. Moreover, the controller starts only at the impact of the system on the ground. The impact is detected according to a condition on the amplitude of the stroke of the suspension. As soon as the stroke of the suspension is positive, the system lands (cf. Figure 7 or Fig. 9). We obtain following results of experiments of semi active device shown in Fig. 12.

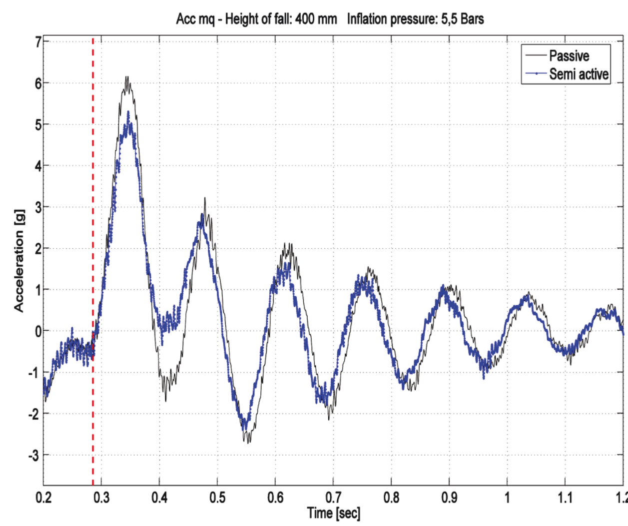

Fig. 12 Measure of acceleration - comparison between passive and semi active system

In Fig. 12, we notice a decrease of 20% on the first peak of acceleration of the upper sprung mass (*mq*) on the semi active system. In comparison with results of simulations of active device on Fig. 11, we can notice that the upper sprung mass (*mq*) continues to oscillate after the shock. This can be explain by the fact that on the semi active system, we only control the damping force of the suspension by tuning throttling section via a proportional servo valve in parallel of the passive hydraulic shock absorber in order to track a target law which is defined by active controller (cf. Figure 11). Thus, we do not add any force via an actuator which is responsible of decrease of oscillations of upper sprung mass (*mq*) after the shock on active device. Nevertheless, semi active device leads to a decrease of amplitude of oscillations of the upper sprung mass (*mq*) at the impact and after the impact.

5 Conclusion

In this paper, a study of induced vibrations by a high speed shock on a complex mechanical system has been presented.

In a first time, analytical and multibody models were designed in order to understand phenomenon. Then cross checking of modeling from measurement on drop test bench has been done, leading to good prediction of dynamic behavior of real system. Following this, an original passive method of minimization of vibrations using mechanical coupling has been developed and experimentally validated. This passive method based on experimental and theoretical coupled approach, consists in design a new characteristic damping law of shock absorber dealing with optimization of the dissipation of energy. This one gives a reduction of 7% on first peak of acceleration of upper sprung mass (*mq*). Finally, different anti vibratory active methods of control have been designed and have been analyzed from numerical simulations. Using mechanical coupling, a sliding mode controller has proved its efficacy in order to minimize the acceleration of an upper system located on an equivalent quarter part of vehicle system submitted to high speed shock. In fact, a reduction of 35% on first peak of acceleration has been predicted.

This control force must be reachable by a dynamical tuning of the damping coefficient of the hydraulic shock absorber. Thus, a semi active device has been designed. This semi active device is composed of controlled proportional servo valve whose supply current is calculate via a inverse model of servo valve whose input is the target control force defined by active controller exposed in this paper. Semi active device using PID controller with minimization of acceleration of mass *mq* as generator of target control force, is experimented. This semi active device is experimented on drop test bench and results are compared to optimal passive device. A decrease of 20% on first peak of acceleration of upper sprung mass (*mq*) has been obtained. These first results are satisfying.

Other active controllers in order to determine target control force have been studied. Ones of those lead to more important decrease of acceleration of the mass *mq*. Thus, semi active device could be improved, using other kind of controllers in order to determine target control force; then these would have to be tested.

A quarter of vehicle is used for passive or active control. It will be however necessary to test the control strategy on the complete vehicle.

Nomenclature

$Gmns$ = center of mass (mns)
Gms = center of mass (ms)
Gq = center of mass (mq)
K_p, a = parameters of PID controller
P = point of contact of the tire
T_d = derivative time constant of PID controller
T_i = integrate time constant of PID controller
$Zmns$ = absolute displacement of the center of mass mns
Zms = absolute displacement of the center of mass ms
Zp = absolute displacement of the point P
Zq = absolute displacement of the center of mass mq
a_i = distance between a center of mass and the point of application of a spring. The index i corresponds to the different notations used in Fig. 1
e = error between desired state and current state
cq = damping coefficient of the upper system
cs = damping coefficient of the suspension
k = tuning parameter of sliding controller
kp = stiffness of the tire
kq = stiffness of the upper system
ks = stiffness of the suspension
$lp0$ = length of the unloaded tire
$lq0$ = length of the unloaded spring kq
$ls0$ = length of the unloaded spring ks
mns = unsprung mass
mq = mass of the upper system
ms = sprung mass
s = sliding surface
u = control force
ε = error between set point and measure
λ = tuning parameter of sliding controller
ξ = damping rate

References

[1] Fischer, D., and Isermann, R., 2004, "Mechatronic Semi Active and Active Vehicle Suspensions," Control Eng. Pract., **12**, pp. 1353–1367.
[2] Lin, J. S., and Kanellakopoulos, I., 1995, "Nonlinear Design of Active Suspensions," 34th IEEE Conference on Decision and Control, New Orleans, LA, Dec. 11–13.
[3] Xu, M., 1997, "Impact Testing and its Applications, Part II," Shock Vib., **29**(4), pp. 8–14.
[4] Kruger, W., 2000, "Integrated Design Process for the Development of Semi-active Landing Gears for Transport Aircraft," Ph.D. thesis, Institut für Flugmechanik und Flugregelung der Universität, Stuttgart.
[5] Ghiringhelli, G. L., 2000, "Testing of Semi Active Landing Gear Control for a General Aviation Aircraft," J. Aircr., **37**(4), pp. 606–616.
[6] Lauwerys, C., Swevers, J., and Sas, P., 2004, "A Flexible Model Free Control Structure for a Semi-active Suspension of a Passenger Car," Proceeding of Intelligent Systems and Control, Honolulu, Hawaii, USA, p. 451.
[7] Der Hagopian, J., Gaudiller, L., and Maillard, B., 1999, "Hierarchical Control of Hydraulic Active Suspensions of a Fast All-Terrain Military Vehicle," Sound Vib., **222**(5), pp. 723–752.
[8] Kirshner, F., Hsu W. C., and Shabana, A. A., 1992, "Effect of the Order of the Finite Element and Selection of the Constrained Modes in Deformable Body Dynamics," Nonlinear Dyn., **3**, pp. 57–80.
[9] Giringhelli, G. L., 2000, "Testing of Semiactive Landing Gear Control for a General Aviation Aircraft, J. Aircr., **37**(4), pp. 606–616.
[10] Giua, A., Melas, M., and Seatzu, C., 2004, "Design of a Control Law for a Semi Active Suspension System Using a Solenoid Valve Damper," Proceeding 2004 IEEE Conference on Control Applications, Taipei, Taiwan.
[11] Guglielmino, E., and Edge, K. A., 2004, "A Controlled Friction Damper for Vehicle Applications," Control Eng. Pract. **12**, pp. 431–443.
[12] Kim, W. S., Lee W. S., and Kim, J. H., 2003, "Control of an Active Vehicle Suspension Using Electromagnetic Motor," Gyeongju, Korea, Oct. 22–25, Paper No. ICCAS2003.
[13] Yagiz, N., 2004, "Comparison and Evaluation of Different Control Strategies on a Full Vehicle Model with Passenger Seat using Sliding Modes," Int. J. Veh. Des., **34**(2), pp. 168–182.